EUROPEAN MECHANICAL SCIENCE

Research Article

e-ISSN: 2587-1110

Erosive-abrasive wear modeling of a water jet pump in a slurry medium

Ergin Kosa[1*], **Yaşar Mutlu**[1]

[1]Istanbul Beykent University, Faculty of Engineering and Architecture, Department of Mechanical Engineering, Istanbul, Türkiye

Abstract: In the study, water jet pump transfers the slurry in the well through pipe system to centrifugal pump. Sand-water mixture causes amount of material loss in the water jet pump structure computed by a software program. The purpose of the study is to determine the most critical part in the water jet pump. The wear amount is affected by many parameters such as sand particle diameter, mass flow rate of abrasive and inlet velocity. So, it is investigated that the wear amount on the jet pump is changed according to sand percentage in the well water, inlet velocity and erodent diameter. Mass flow rates of sand have a value of 0.097 kg/s for w.p. % 5, 0.194 kg/s for w.p. % 10, 0.291 kg/s for w.p. % 15 at an inlet velocity of 3.98 m/s. The maximum erosion wear rate is raised from $2.26x10^{-4}$ kg/(s m^2) to $6.84x10^{-8}$ kg/s^2m^2 for inlet velocities of 1.99 m/s, 3.98 and 7.96 m/s, respectively for the case of weight percentages of %15 in Finnie erosion wear model. Finnie, Mclaury, Generic and Oka erosion models have been compared. It is found that Mclaury's erosion model demonstrates the highest erosion value of $1.38x10^{-3}$ kg/(s m^2) for w.p. % 15 at 3.98 m/s inlet velocity for the erodent diameter of 0.0005m in all. It is claimed that erosive wear has been concentrated on the nozzle of the water jet pump. The wear rate can be predicted as straightforwardly for different conditions.

Keywords: Erosion-abrasive wear, Modeling, Water Jet Pump, Slurry, Flow

1. Introduction

Erosive-abrasive wear is caused by the solid particles carried by liquid [1-7]. It is prevalently formed in transportation systems such as pumps, pipes, turbines and valves [6,8-10]. Fine abrasive particles are transferred in the fluids in the field of industry such as oil [11,12], gas production [13] or in engineering applications such as dewatering and dredging [14]. These fine particles in the fluids are primary cause of wear in the transportation system components such as water jet pump providing simple structure without a movable part [15] or in a slurry mixed container [16,17] or in a turbine [18-20]. The water jet pump is used to transmit fluid at low speed from narrow deep wells when the water level is too low for a normal pump suction head to operate and a primary flow is named as motive flow diverged from the total volume flow in the pump [15,21-23]. The primary flow is recirculated to the jet pump which is mounted under the lowest water level [24].

Erosion wear is commonly investigated in pipe systems [11,12,25]. The researchers concentrated on the wear in pipe elbows because of the change in flow direction[11,12,25, 26]. The novelty of the research is that the study is focused on the erosive wear of water jet pump transferring slurry mixture in the well. The sand-water slurry mixture removes material on the parts of water jet pump such as nozzle, mixing part and diffuser because of continuous impingement of the abrasive sand particles. The effects of inlet speed, particle size and particle amount on the wear were studied in a software program and the results are discussed herein. The critical parts of this water jet pump such as nozzle, mixing and diffuser regions have not been discussed in terms of slurry erosion in the literature yet. Computational analysis of slurry erosion model is the straightforward method to provide the determination of critical points in the water jet pump, maintenance and protection of them.

Some researchers studied on erosion wear in literature. Kosinska et al studied on erosion of pipe elbow for different particle diameters from nano to micro size and fluid velocity. Although, the erosion rate for under the

*Corresponding author:
Email: erginkosa@beykent.edu.tr

Cite this article as:
Kosa, E., Mutlu, Y.(2024). Erosive-abrasive wear modeling of a water jet pump in a slurry medium.*European Mechanical Science*, 8(4):257-266.https://doi.org/10.26701/ems.1504033

History dates:
Received: 24.06.2024, *Revision Request*: 12.07.2024, *Last Revision Received*: 22.08.2024, *Accepted*: 22.08.2024

erodent diameter of 10^{-6}m decreases with particle size, nano particles cause clustering to form local erosion [27]. Doroshenko et al numerically analyzed worn-tee of the main gas pipeline withstanding additional stresses due to gas stream action. It is found that the maximum Mises equivalent stresses in the tee caused by the erosion wear of its line wall are formed on the outside of the tee line near the reinforcing lining located on the tee line [28]. Bai et al investigated erosion wear of helicopter rotor blades made up of titanium alloy, magnesium alloy, or aluminum alloy the construction material, respectively. It is found that Ti-4Al-1.5Mn alloy performs the highest erosion resistance. The erosion rates of the three materials remained nearly unchanged with changes in the angle of attack [29]. Yan et al (2020) modeled erosion wear in the hydraulic amplifier of the deflector jet servo valve influenced by abrasives in the oil. CFD simulation and Oka erosion model were used to emphasize the wear on the amplifier. It is claimed that the major erosion wear happens on the shunt wedge [30]. Yanan and Tingzhou numerically simulated computational fluid mechanics in 3 different types of elbows and experimentally tested the erosion wear performance of the elbows. Yanan and Tingzhou found that the elbow made up of 42CrMo material demonstrates the highest resistance to erosion wear in all [31]. Kannojiya and Kumar designed slurry pipe having a different bending angle to minimize the worn material on the pipe surface and focused on the velocity in the pipes having 150 mm diameter and 250 mm diameters. It is seen that increase in velocity can maximize wear amount and high bending angles provide to lower rate of erosion [32]. Kumar et al studied on effect of swirl vanes angle on erosion wear of AISI 316 pipe. Pipe model with vanes having different swirl angles and without a vane was compared in terms of erosion rate. Kumar *et al* claimed that placing a swirl vane enables reduce in the erosion rate on the pipe bend for all cases studied except when a 30° swirl vane was mounted at 360 mm from the inlet of the upstream pipe. Also, As the swirl angle is decreased, the erosion wear across bend is also decreasing [33]. Farokhipour et al. modeled sand particle erosion in gas-solid particle two phase flow at sharp bend, standard elbow, long elbow, and 180° pipe bend. Particle sizes of 150 and 300 μm were considered in the study of Farokhipour et al [34].

2. Mathematical Model of Flow

Pandhare and Pitale designed water jet pump parametrically. In the study, this water jet pump model [21] was modified and used in an irrigation system for transporting water and sand particles at low weight percentage as depicted in ▶**Figure 1**. The sand particles inside the water strike the inner surface of jet pumps during flow. The cyclic impact is the reason of material removal in the jet pump. Thus, action of the slurry mixture causes wear in the jet pump. The jet pump dimensions in units of mm have been illustrated in ▶**Figure 2**.

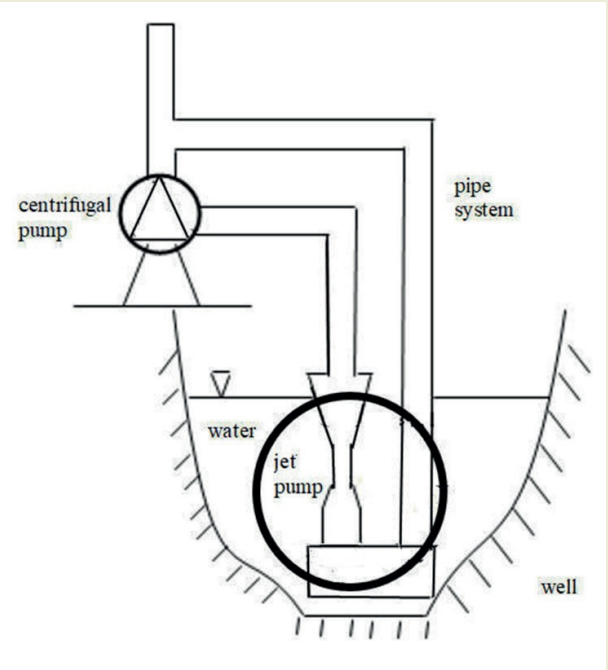

Figure 1. Irrigation system

2.1. Jet Pump Model

The water jet pump investigated for the current study consists of a diffuser and nozzle. RANS turbulence model was applied. The turbulent k-ω-SST was chosen as the flow model inside the water jet pump. Due to the

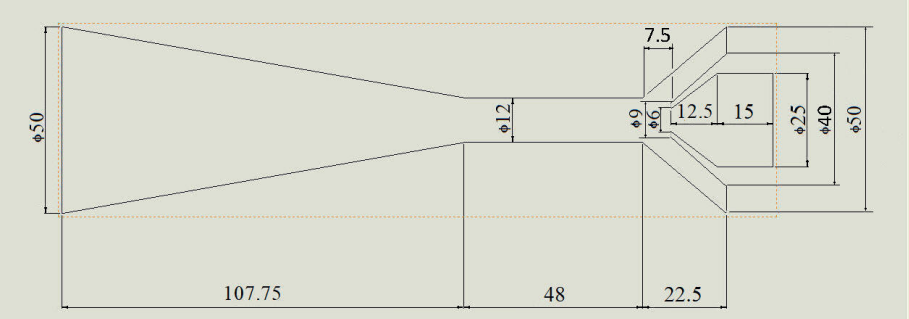

Figure 2. Water Jet Pump Dimensions

fact that the k-ω (SST) model utilizes both benefits of k-w and k-ε models. The k-w model demonstrates accurate results in the near wall, whereas k-ε models in the far-field region. So, the k-ω (SST) model can provides a wide range of accurate flow profiles [35].

The RANS momentum and continuity equations were used in computation. In physical model incompressible flow was activated. The flow analysis was realized at different velocities to emphasize the flow character inside the pump. It was performed at velocities of 1.99 m/s, 3.98 m/s and 7.96 m/s for representing low operating speeds, respectively. The other boundary conditions are given in ▶Table 1. On the other hand, the magnitude of velocity is one of the main effective parameters in erosion wear in slurry medium. In addition to turbulent flow model, particle tracing model for fluid flow was run to investigate erosion wear behavior of slurry mixture on the water jet pump design. The particle density of sand is specified as 2200 kg/m^3. The erosion rate on the surface of water jet pump was investigated and particle trajectory was simulated according to time. The model was run for 15s as illustrated in ▶Figure 3 and Δt is set as 0.01 s.

2.2. CFD Model of Flow

Continuity equation in water jet pump is defined in Equations 1-3 as;

$$Q_{total} = Q_{pri} + Q_{\sec} \tag{1}$$

$$A_{total}V_{total} = A_{pri}V_{pri} + A_{\sec}V_{\sec} \tag{2}$$

$$\pi\frac{(d^2_{total})}{4}V_{total} = \pi\frac{(d^2_{pri})}{4}V_{pri} + \pi\frac{(d^2_o - d^2_i)}{4}V_{\sec} \tag{3}$$

Turbulent flow model [36]:

The mathematical expression of incompressible flow in steady state is defined in Equations 4-9 as;

$$\rho(u.\nabla)u = \nabla\left[-pl + (\mu + \mu_T)\left(\nabla u + (\nabla u)^T\right)\right] \tag{4}$$

$$\rho\nabla(u) = 0 \tag{5}$$

$$\rho(u.\nabla)k = \nabla\left[(\mu + \mu_T\sigma^*_k)\nabla k\right] + p_k - \beta^*_o\rho\omega k \tag{6}$$

Table 1. Boundary conditions for inlets

Parameters	Value
Particle density, ρ_p	2200 kg/m^3
Mass flow rate, $\dot{m}$	0.097 kg/s-0.388 kg/s
Initial particle diameter	0.0001 m-0.00025 m-0.0005m-0.00025m-0.001m
Normal inflow velocity, U	1.99-3.98-7.96 m/s

$$\rho(u.\nabla)k = \nabla[(\mu + \mu_T\sigma_\omega)\nabla\omega] + \alpha\tfrac{\omega}{k}p_k - \beta_0\rho\omega^2, \omega = om \tag{7}$$

and the turbulent viscosity are denoted as;

$$\mu_T = \rho\frac{k}{\omega} \tag{8}$$

the production term is expressed as;

$$p_k = \mu_T[\nabla u : (\nabla u + (\nabla u^T)]) \tag{9}$$

3. Mathematical Model of Erosion

3.1. Particle Tracing

The particle tracing for fluid flow was run to analyse particle trajectory in jet pump as illustrated in ▶Figure 3. The abrasive sand particles from different inlets are mixed at the end of nozzle part. The abrasive sand particles start to move along the jet pump and reach to outlet at the end. The inlet velocity of particles is 3.98 m/s along the jet pump axial direction. The computation according to time was run for the case of erodent size diameter of 500 µm and % 10 weight percentage slurry mixture.

3.2. Erosion Prediction

The mass flow rates of sand particles in slurry were varied from 0.097 kg/s to 0.388 kg/s. Those values are relatively low intensities. Thus, it is assumed that Newtonian flow is formed in water jet pump. The sand particles inside water jet pump cause an amount of material to be removed. The four erosion models are used to analyze the erosion behavior in the water jet pump. These are Finnie, Mclaury, Generic and Oka models that are selected in program. Mathematical expressions of these three erosion models are as follows;

3.2.1 Finnie Erosion Model [37]

Impact angle and velocity are principal factors affecting the wear in the Finnie model as expressed in Equation 10.

$$ER_{Finnie} = \sum_{p=1}^{N}\frac{\dot{m}_p Lf(\alpha)v_p^{vel}}{A_{face}} \tag{10}$$

3.2.2 The Mclaury Model [38]

The McLaury erosion model computes the erosion rate of solid particles in slurry and is shown in Equations 11,12.

$$ER_{Mclaury} = GBh^jV^{vel}f(\gamma) \tag{11}$$

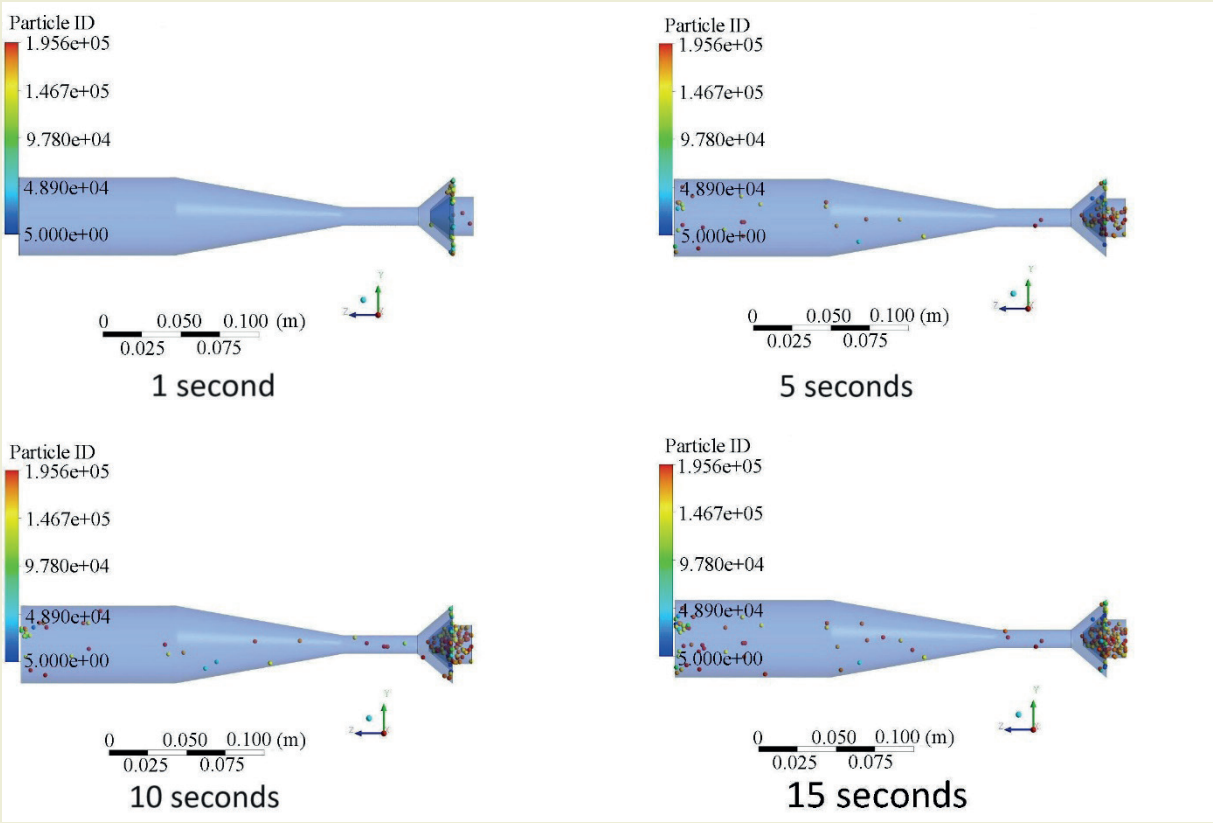

Figure 3. Particle trajectories in water jet pump-U=3.98 m/s After 1s, 5s, 10s, 15s.

$$f(\gamma) = \begin{cases} b\gamma^2 + c\gamma & \gamma \le \gamma_{\lim} \\ x\cos^2(\gamma)\sin(w\gamma) + y\sin^2\gamma + z & \gamma_{\lim} < \gamma \end{cases} \quad (12)$$

3.2.3 Oka Model [39, 40]

Oka model calculates erosion rate in Equations 13 as;

$$E_f = \frac{1}{A_f}\sum_i \dot{m}_d\,(sin\alpha)^{n_1}(1 + Hv(1-\sin\alpha))^{n_2} K\left(\frac{V_{rel}}{V_{ref}}\right)^{k_2}\left(\frac{D}{D_{ref}}\right)^{k_3} \quad (13)$$

3.2.4 Generic Model [41]

The generic model is developed by Hamed *et al* and is focused on the erodent's size, impact angle and impact velocity. The Generic model is expressed in Equation 14.

$$ER_{Generic} = \sum_{p=1}^{Ntrajct} \frac{m_{pfr} C(d_p) f(\alpha) v_p^{vel}}{A_{face}} \quad (14)$$

4. Results and Discussion

The investigated regions in the jet pump are illustrated in ▶**Figure 4**. The mixing region, diffuser and inlets of nozzle are depicted in ▶**Figure 4**. Outlet pressure is 100000 Pa. Pressure inlet is 0 Pa.

Mesh test was done for different number of mesh elements to determine the adequate number of elements to solve the model analysis and to get a much more accurate results as shown in ▶**Table 2**. The analysis resulted in magnitude of maximum Finnie wear rates in water jet pump and erosive wear values on water jet pump are changing approximately within 0.46 % deviation for 7070000 number of mesh elements and 44000000 number of mesh elements. Thus, it is determined that the 7070000 number of mesh elements is adequate to be used to solve 3-D erosion wear model. Inflation layer is 5. Infilation thickness is 0.005. Mesh size is 0.75.. Tetrahedral grid elements are adopted within the computational domain. Also, for capturing of near wall flow treatment, high gradient mesh structure is used along the walls. For this propose an inflation with first layer thickness of $5x10^{-3}$ mm and growth rate of 1.2 for 5 layers is applied to all walls. Accordingly, the enhanced

Table 2. Mesh dependence test

Number	Number of Mesh Elements	Finnie max. wear rates Velocity (m/s)
1	1100000	0.000320
2	3010000	0.000380
3	7070000	0.000430
4	23000000	0.000432
5	44000000	0.000432

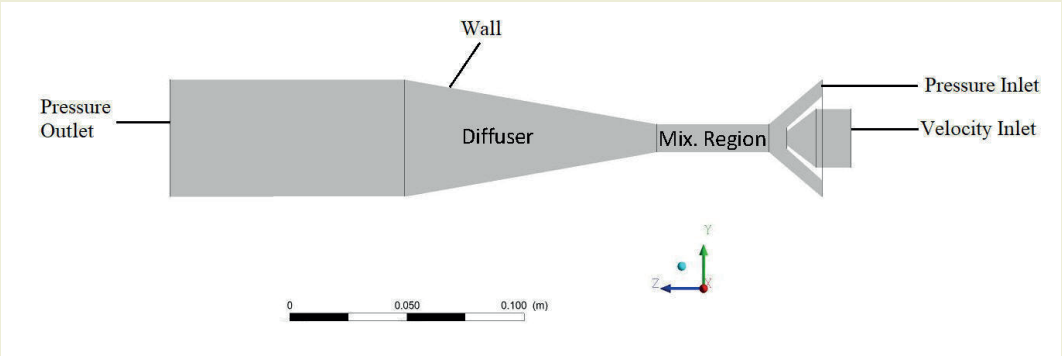

Figure 4. Regions on the water jet pump

wall treatment approach is implemented for turbulence modeling. The computational domain and the details of the mesh are shown in ▶**Figure 5**.

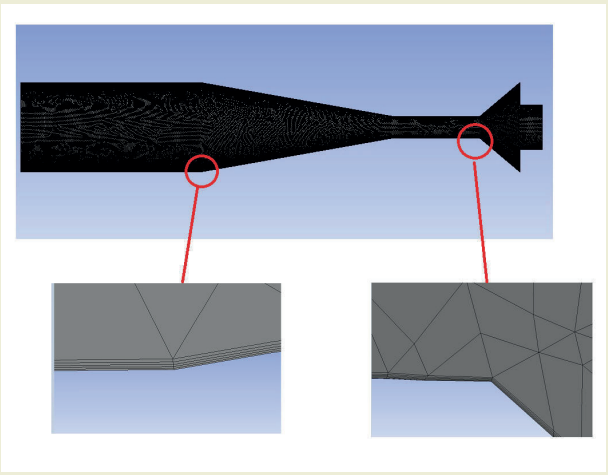

Figure 5. Mesh of model

4.1. Effect of Medium Parameters on Wear Rate

Erosive wear in jet pump depends on some parameters such as speed, slurry mass flow rate, diameter of abrasive particle. These parameters are called as medium conditions in jet pump. Thus, in the study, effect of these parameters inside the jet pump was investigated.

4.1.1 Influence of Sand Amount on Erosion Wear of Water Jet Pump

The weight percentages of sand in the slurry mixture were varied from % 5-%15 for all erosion wear models. The maximum erosion wear rate of Mclaury wear model increased from 4.54×10^{-4} kg/(s m^2) to 13.8×10^{-4} kg/(s m^2) for the wps from %5 - %15 as shown in ▶**Figure 6**. The maximum erosion wear rates in Finnie wear model were reached up to values of 6.84×10^{-4} kg/(s m^2), 4.30×10^{-4} kg/(s m^2), 2.26×10^{-4} kg/(s m^2) for the slurry mixtures of % 5, %10 and %15 weight percentages as illustrated in ▶**Figure 6**. Maximum wear rates in Oka models are 0.936×10^{-5} kg/(s m^2), 1.80×10^{-4} kg/(s m^2), 2.83×10^{-4} kg/(s m^2) for % 5, %10 and %15 weight percentages as depicted in ▶**Figure 6**. Generic models demonstrate the lowest wear rates in all erosion wear models. The maximum wear rates achieved to 11.3×10^{-4} kg/(s m^2), 7.5×10^{-4} kg/(s m^2), 3.75×10^{-4} kg/(s m^2) for % 5, %10 and %15 weight percentages of sand in slurry. The maximum erosion wear rates increase linearly according to weight percentages of sand in slurry in the water jet pump as illustrated in ▶**Figure 6**.

4.1.2 Influence of Abrasive Particle Diameters on Erosion Wear of Water Jet Pump

The effect of the erodent size on the erosion wear was studied in the work. As the particle size decreased from 0.0005 m to 0.001 m, the erosion wear rate increased as depicted in ▶**Figure 7**. In contrast, the wear rate increased from 4.30×10^{-4} kg/(s m^2) to 1.19×10^{-2} kg/(s m^2) for the case of Finnie wear model, from 7.50×10^{-4} kg/(s m^2) to 6.66×10^{-2} kg/(s m^2) for the case of Generic wear model, from 8.65×10^{-4} kg/(s m^2) to 1.66×10^{-2} kg/(s m^2) for the case of Mclaury wear model, from 1.80×10^{-4} kg/(s m^2) to 6.22×10^{-3} kg/(s m^2) for the case of Oka model. This demonstrates that the smaller abrasives were be-

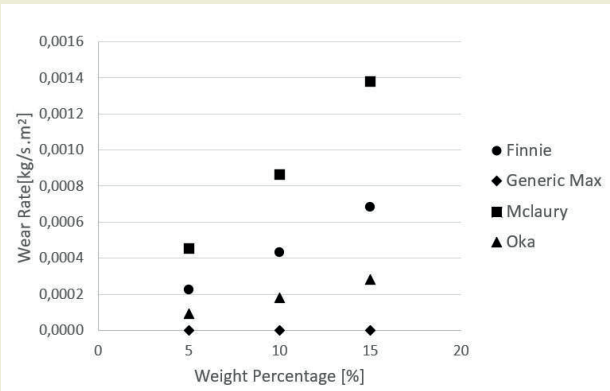

Figure 6. Wear rate for different weight percentages for each erosive wear model.

https://doi.org/10.26701/ems.1504033

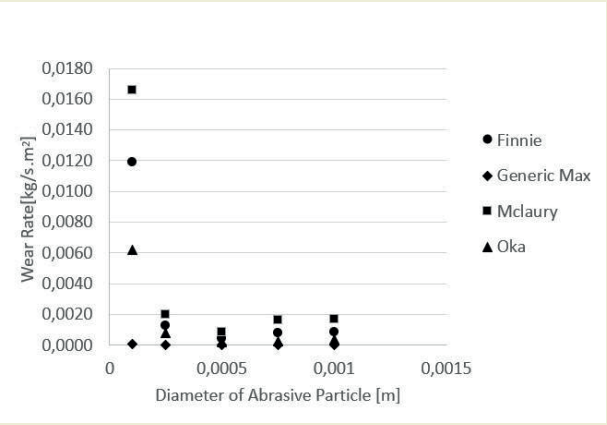

Figure 7. Wear rate under impacting of different abrasive diameter for different erosive wear models.

ing pulled towards the nozzle wall resulting in higher erosion wear.

The region for the case of smaller erodent diameter of 0.00025 m in ▶**Figure 8a** is greater than the case of 0.0005 m as depicted in ▶**Figure 8b**. The regions of higher erosion wear values were enlarged as the erodent diameter was increased from 0.0005 m to 0.001 m as shown in ▶**Figures** of **8b, 8c** and **8d**.

4.1.2 Influence of Flow Velocity on Erosion Wear of Water Jet Pump

The influence of inlet flow velocity on maximum erosion wear was investigated. The wear rate increases increasingly for all erosion wear models as shown in ▶**Figure 9**. The maximum wear rates on the nozzle of the water jet pump reached to $1.2x10^{-4}$ kg/(s m^2), $4.3x10^{-4}$ kg/(s m^2) and $3.92x10^{-3}$ kg/(s m^2) according to Finnie model for the inlet velocities of 1.99 m/s, 3.98 m/s, 7.96 m/s, respectively; $4.10x10^{-7}$ kg/(s m^2), $7.5x10^{-7}$ kg/(s m^2), $1.51x10^{-6}$ kg/(s m^2) according to the Generic model for the inlet velocities of 1.99 m/s, 3.98 m/s, 7.96 m/s, respectively; $2.3x10^{-4}$ kg/(s m^2), $8.65x10^{-4}$ kg/(s m^2), $6.78x10^{-3}$ kg/(s m^2) according to Mclaury model for the inlet velocities of 1.99 m/s, 3.98 m/s, 7.96 m/s, respectively; from $5.7x10^{-5}$ kg/(s m^2), $1.80\ x10^{-4}$ kg/(s m^2), $1.89x10^{-3}$ kg/(s m^2) according to Oka model for the inlet

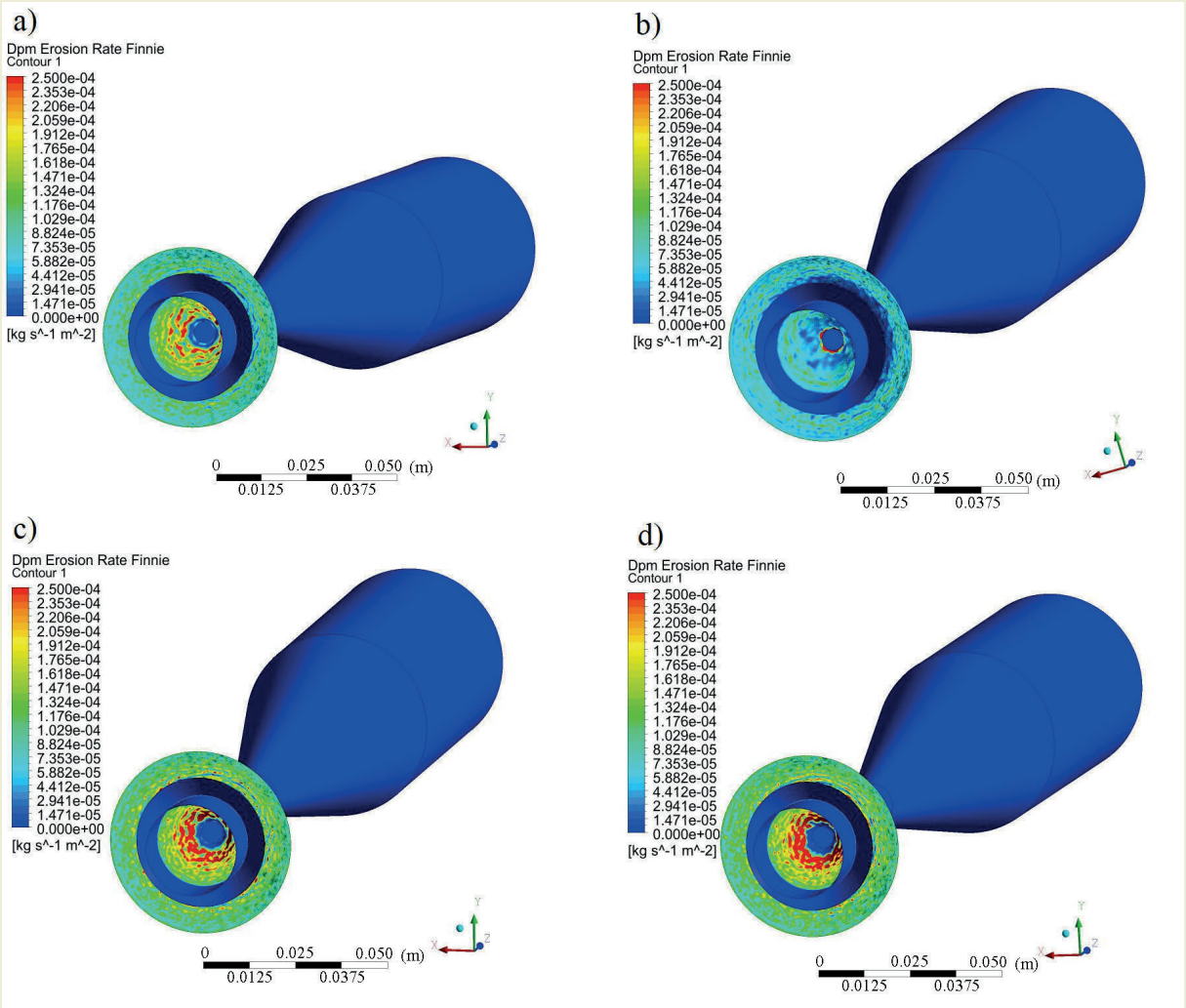

Figure 8. Erosion wear rates for different erodent diameters.

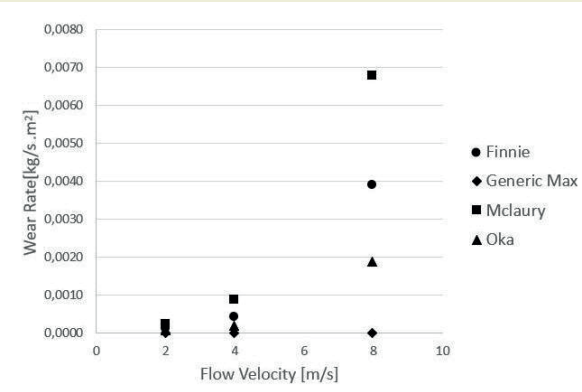

Figure 9. Wear rate at different flow velocities for different erosive wear models.

velocities of 1.99 m/s, 3.98 m/s, 7.96 m/s, respectively.

Erosion wear rate was focused on the lateral surface of the nozzle at velocity of 3.98 m/s as depicted in ▶**Figure 10b**. As the velocity increased from 3.98 m/s in ▶**Figure 10a** to 7.96 m/s in ▶**Figure 10c**, the higher values of erosion wear were concentrated around the nozzle exit as illustrated in ▶**Figure 10d**. In ▶**Figure 10a** and **c**, it is illustrated that flow is separated at certain point inside the diffuser part of water jet pump due to the turbulence.

4.2. Comparison of Erosion Wear Models

Erosion wear rates of four different wear models of Finnie, Mclaury, Oka and Generic were computed in the water jet pump as illustrated in ▶**Figure 11**. The maximum wear rates in Finnie, Oka and Mclaury have been evaluated inner part of the nozzle while the maximum wear rate has been achieved in outer part of the nozzle for Generic model.

5. Conclusion

The water jet pump was analyzed to identify the possible leakage locations due to impacting particles in slurry medium. The amount of sand particles affected the erosion rate inside the water jet pump directly. The wear rates were evaluated to determine maximum val-

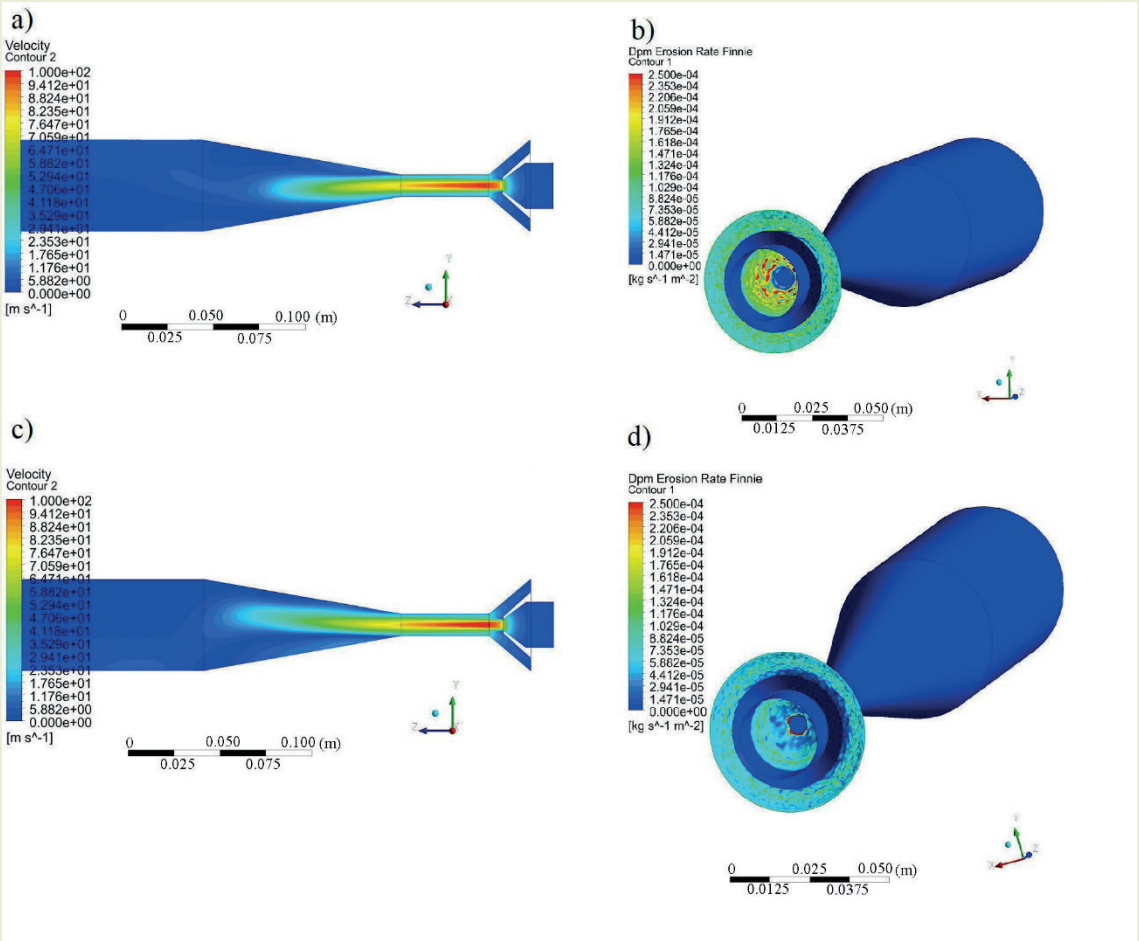

Figure 10. Erosion Wear Rate For Different Velocities.

https://doi.org/10.26701/ems.1504033

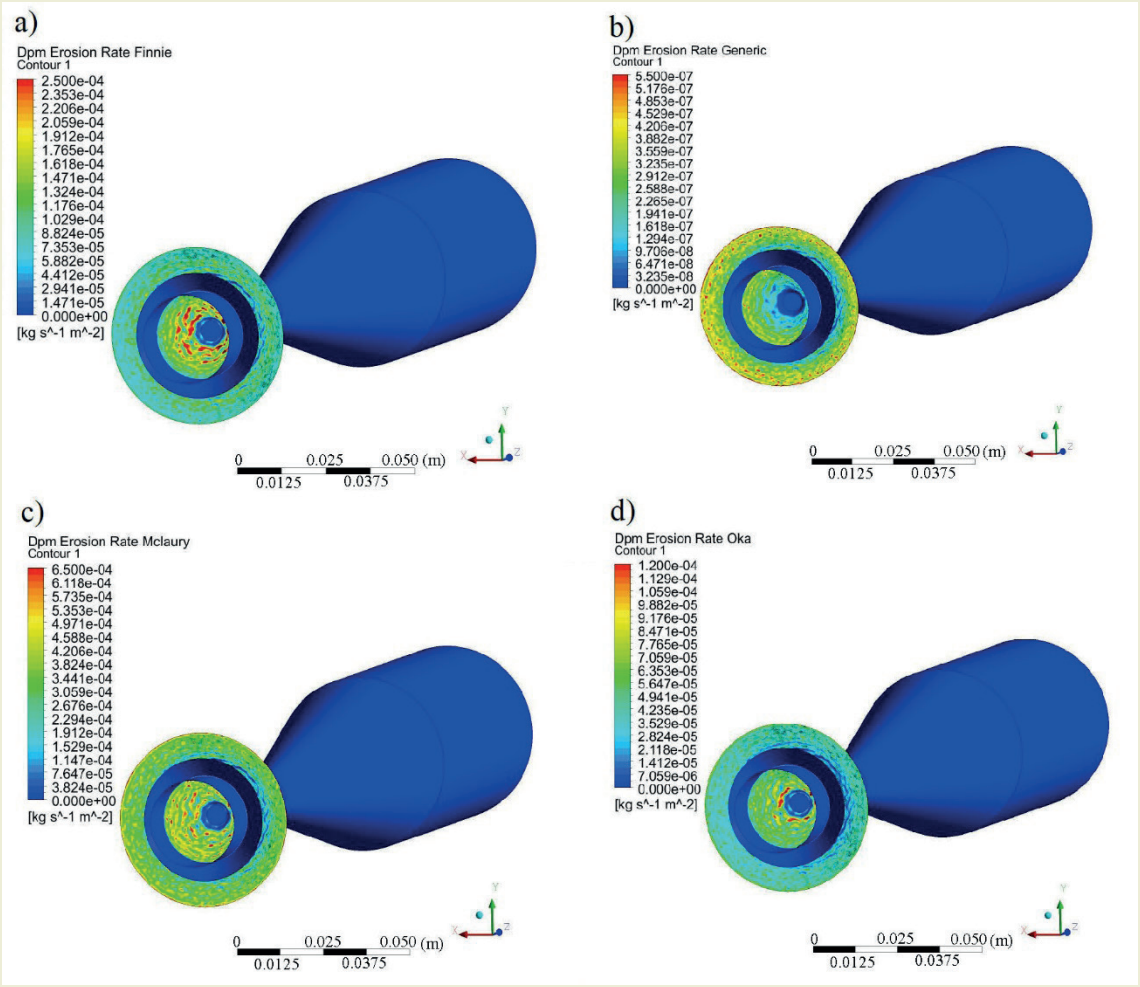

Figure 11. Finnie, Generic, Mclaury, OKA erosion rates in water jet slurry pump.

ues expressing the critical region of the water jet pump. The most affected area by the erosive wear is the nozzle of the water jet pump. This situation was approached with 4 erosive wear models.

It was concluded that all models showed that the wear rate increases when the slurry percentage in weight increases, and likewise for all modeling approaches the increase in erosion wear rate demonstrates similar tendency when the input speed and abrasive size increases. Mclaury Finnie, Oka and Generic erosive wear model values for the erodent diameter of 0.0001m results in the highest erosive rates of 1.66×10^{-2} kg/(s m^2), 1.19×10^{-2} kg/(s m^2), 6.22×10^{-3} kg/(s m^2), 6.66×10^{-5} kg/(s m^2) at the inlet velocity of 3.98 m/s in the % 10 w.p. slurry medium, respectively.

It has been also computed that increase in abrasive mass flow rate, abrasive size, particle speed increase the wear rate. Thus, the wear rate can be estimated as straightforwardly for various cases. It is significant, because gradually increase in wear amount in the water jet pump lowers the performance of water the jet pump. The indicated critical points on the nozzle can be coated as a material that are more resist to erosive wear to minimize wear rate.

Nomenclature

Q_{pri} : Primary flow (m^3 s^{-1})
Q_{sec} : Secondary flow (m^3 s^{-1})
Q_{total} : Total flow (m^3 s^{-1})
A_{pri} : Section area of primary flow (m^2)
A_{sec} : Section area of secondary flow (m^2)
V_{sec} : Velocity of secondary flow (m s^{-1})
V_{pri} : Velocity of primary flow (m s^{-1})
d_o : Outer diameter (m)
d_i : Inner diameter (m)
d_{pri} : Primary diameter (m)
d_{total} : Total diameter (m)
V_{total} : Total velocity (ms^{-1})
ρ : The fluid density (kg m^{-3})
ρ_p : *Density of particle (kg m^{-3})*

u: The fluid velocity (m s^{-1})
p: The fluid pressure (Pa)
$\dot{m}$: Mass flow rate (kg s−1)
μ_T : The modified eddy (or turbulent) viscosity (Pa s)
P_k : Rate of production of turbulent kinetic energy (m^2s^{-2})
H_v : Vickers hardness of material (HVN)
B_h : Brinell hardness of material
μ: Fluid viscosity (Pa s)
U: Inlet velocity (m s^{-1})
V: The velocity of the impacting particle (m s^{-1})
γ: The impact angle
ER_{Finnie} : The erosion rate (kg $s^{-1}m^2$)
$ER_{Mclaury}$: The erosion rate (kg $s^{-1}m^2$)
E_f: The erosion rate (kg $s^{-1}m^2$)
$ER_{Generic}$: The erosion rate (kg $s^{-1}m^2$)
f(γ): The function of the impact angle
γ_{lim} : The transition angle
b: Experimentally derived constant
c: Experimentally derived constant
w: Experimentally derived constant
x: Experimentally derived constant
y: Experimentally derived constant
z: Experimentally derived constant
m_{pfr} : Mass flow rate of the particles
$C(d_p)$: Concentration function in terms of the particle diameter
v_p : The particle impact velocity (m s^{-1})
vel: The velocity exponent
$\dot{m}_p$: The mass flow rate of the impact stream
f(α): An impact angle function
α: An impact angle (rad)
N: The number of particles
A_{face} : The impact area (m^2)
j: Constant
L: Constant
n_1 : Constant
n_2 : Constant
G : Constant
k_2 : Constant
k_3 : Constant
K : Constant
v_{rel} : The relative velocity of the particle with respect to the wall (m s^{-1})
v_{ref} : The reference value for velocity (m s^{-1})
D: Particle diameter (m)
D_{ref} : The reference value for diameter (m)
$\dot{m}d$: The mass flow rate of particles colliding with the surface (kg s^{-1})

Research Ethics

Ethical approval not required.

Author Contributions

The authors accept full responsibility for the content of this article and have approved its submission.

Competing Interests

The author(s) declare that there are no competing interests.

Research Funding

Not reported.

Data Availability

Not applicable.

Orcid

Ergin Kosa https://orcid.org/0000-0002-4607-4115
Yaşar Mutlu https://orcid.org/0000-0002-5460-5609

References

[1] Islam, M. A., & Farhat, Z. N. (2014). Effect of impact angle and velocity on erosion of API X42 pipeline steel under high abrasive feed rate. *Wear, 311,* 180–190. https://doi.org/10.1016/j.wear.2014.01.005

[2] Jerman, M., Zeleňák, M., Lebar, A., Foldyna, V., Foldyna, J., & Valentinčič, J. (2021). Observation of cryogenically cooled ice particles inside the high-speed water jet. *Journal of Material Processing Technology, 289,* 116947. https://doi.org/10.1016/j.jmatprotec.2020.116947

[3] Kosa, E., & Göksenli, A. (2015). Effect of impact angle on erosive abrasive wear of ductile and brittle materials. *International Journal of Mechanical, Aerospace, Industrial, Mechatronic and Manufacturing Engineering, 9,* 536-540. http://scholar.waset.org/1307-6892/10002428

[4] Sheng, M., Huang, Z. W., Tian, S. C., Zhang, Y., Gao, S-W., & Jia, J-P. (2020). CFD analysis and field observation of tool erosion caused by abrasive waterjet fracturing. *Petroleum Science, 17(3),* 701-711. https://doi.org/10.1007/s12182-020-00425-1

[5] Zhang, L., Ji, R., Fu, Y., Qi, H., Kong, F., Li, H., & Tangwarodomnukun, V. (2020). Investigation on particle motions and resultant impact erosion on quartz crystals by the micro-particle laden waterjet and airjet. *Powder Technology, 360,* 452-461. https://doi.org/10.1016/j.powtec.2019.10.032

[6] Zhang, R., Liu, H., & Zhao, C. A. (2013). Probability model for solid particle erosion in a straight pipe. *Wear, 308,* 1–9. https://doi.org/10.1016/j.wear.2013.09.011

[7] Zhao, Y. L., Tang, C. Y., Yao, J., Zeng, Z.-H., & Dong, S.-G. (2020). Investigation of erosion behavior of 304 stainless steel under solid–liquid jet flow impinging at 30°. *Petroleum Science, 17,* 1135–1150. https://doi.org/10.1007/s12182-020-00473-7

[8] Guo, B., Li, Y. H., Xiao, Y. X., Ahn, S. H., Wu, X., Zeng, C. J., & Wang, Z. W. (2021). Numerical analysis of sand erosion for a Pelton turbine injector at high concentration. *Earth and Environmental Science,* 627, 012022.

[9] Safaei, M. R., Mahian, O., Garoosi, F., Hooman, K., Karimipour, A., Kazi, S. N., & Gharehkhani, S. (2014). Investigation of micro- and nanosized particle erosion in a 90° pipe bend using a two-phase discrete phase model. *The Scientific World Journal.* https://doi.org/10.1155/2014/740578

[10] Vieira, R. E., Mansouri, A., McLaury, B. S., & Shirazi, S. A. (2016). Experimental and computational study of erosion in elbows due to sand particles in air flow. *Powder Technology, 288,* 339–353. https://doi.org/10.1016/j.powtec.2015.11.028

[11] Al-Baghdadi, M. A., Resan, K. K., & Al-Wail, M. (2017). CFD investigation of the erosion severity in 3D flow elbow during crude oil contaminated sand transportation. *Engineering and Technology Journal, 35,* 930–935. https://doi.org/10.30684/etj.35.9A.10

[12] Sanni, S. E., Olawale, A. S., & Adefila, S. S. (2015). Modeling of sand and crude oil flow in horizontal pipes during crude oil transportation. *Journal of Engineering,* 1–7. https://doi.org/10.1155/2015/457860

[13] Parsi, M., Najmi, K., & Najafifard, F. A. (2014). Comprehensive review of solid particle erosion modeling for oil and gas wells and pipelines applications. *Journal of Natural Gas Science and Engineering, 21,* 850–873. https://doi.org/10.1016/j.jngse.2014.10.001

[14] El-Sawaf, I. A., Halawa, M. A., Younes, M. A., & Teaima, I. R. (2011). Study of the different parameters that influence on the performance of water jet pump. *Fifteenth International Water Technology Conference,* Egypt.

[15] Song, X. G., Park, J. H., Kim, S. G., & Park, Y. C. (2013). Performance comparison and erosion prediction of jet pumps by using a numerical method. *Mathematical and Computer Modelling, 57,* 245–253. https://doi.org/10.1016/j.mcm.2011.06.040

[16] Jafari, A., & Abbasi, H. R. (2020). Investigation of parameters influencing erosive wear using DEM. *Friction, 8(1),* 136–150. https://doi.org/10.1007/s40544-018-0252-4

[17] Murugan, K., & Karthikeyan, S. (2018). CFD modelling, analysis and validation of slurry erosion setup with naval brass. *JAC: A Journal of Composition Theory, 11(10),* 63-72.

[18] Finn, J. R., & Doğan, Ö. N. (2019). Analyzing the potential for erosion in a supercritical CO2 turbine nozzle with large eddy simulation. *Turbomachinery Technical Conference and Exposition.* American Society of Mechanical Engineers Digital Collection. https://doi.org/10.1115/GT2019-91791

[19] Castorrini, A., Corsini, A., Rispoli, F., Venturini, P., Takizawa, K., & Tezduyar, T. E. (2019). Computational analysis of performance deterioration of a wind turbine blade strip subjected to environmental erosion. *Computational Mechanics, 64(4),* 1133-1153. https://doi.org/10.1007/s00466-019-01697-0

[20] Qian, Z., Zhao, Z., Guo, Z., Thapa, B. S., & Thapa, B. (2020). Erosion wear on runner of Francis turbine in Jhimruk Hydroelectric Center. *Journal of Fluids Engineering, 142(9).* https://doi.org/10.1115/1.4047230

[21] Pandhare, S. R., & Pitale, A. K. (2017). Study the performance of water jet pump by changing the angle of mixing nozzle. *International Journal of Scientific Research in Science and Technology, 3(3),* 538.

[22] Pitale, A. K., & Pandhare, S. R. (2017). Experimental investigation of jet pump at different nozzle-to-throat spacing to nozzle diameter ratio (X). *International Journal of Scientific Research in Science and Technology, 3(4),* 168-171.

[23] Sheha, A. A. A., Nasr, M., Hosien, M. A., & Wahba, E. (2018). Computational and experimental study on the water-jet pump performance. *Journal of Applied Fluid Mechanics, 11(4),* 1013-1020. https://doi.org/10.29252/jafm.11.04.28407

[24] Sakuragi, S., & Zhao, S. (2018). Operating characteristics of multi-injection type underwater jet pump. *American Journal of Mechanics and Applications, 6(3),* 68-77.

[25] Yam, K. S., Roy, S., Lee, V. C. C., & Law, M. C. (2020). Numerical analysis of erosion pattern on pipe elbow bend with swirling flows. *2nd International Conference on Materials Technology and Energy, IOP Conference Series: Materials Science and Engineering, 943,* 012037. https://doi.org/10.1088/1757-899X/943/1/012037

[26] Banakermani, M. R., Naderan, H., & Saffar-Avval, M. (2018). An investigation of erosion prediction for 15° to 90° elbows by numerical simulation of gas-solid flow. *Powder Technology, 334,* 9–26. https://doi.org/10.1016/j.powtec.2018.04.033

[27] Kosinska, A., Balakin, B. V., & Kosinski, P. (2020). Theoretical analysis of erosion in elbows due to flows with nano- and micro-size particles. *Powder Technology, 364,* 484–493. https://doi.org/10.1016/j.powtec.2020.02.002

[28] Doroshenko, Y., Zapukhliak, V., Grudz, Y., Poberezhny, L., Hrytsanchuk, A., & Popovych, P. (2020). Numerical simulation of the stress state of an erosion-worn tee of the main gas pipeline. *Archives of Material Science and Engineering, 101,* 63-78. https://doi.org/10.5604/01.3001.0014.1192

[29] Bai, X., Yao, Y., Han, Z., Zhang, J., & Zhang, S. (2020). Study of solid particle erosion on helicopter rotor blades surfaces. *Applied Sciences, 10(3),* 977. https://doi.org/10.3390/app10030977

[30] Yan, H., Li, J., Cai, C., & Ren, Y. (2020). Numerical investigation of erosion wear in the hydraulic amplifier of the deflector jet servo valve. *Applied Sciences, 10(4),* 1299. https://doi.org/10.3390/app10041299

[31] Yanan, G., & Tingzhou, N. (2020). Numerical simulation and experiment analysis on erosion law of fractured elbow pipe. *Academic Journal of Manufacturing Engineering, 18(2),* 109-115.

[32] Kannojiya, V., & Kumar, S. (2020). Assessment of optimum slurry pipe design for minimum erosion. *Scientia Iranica, 27(5),* 2409-2418. https://doi.org/10.24200/SCI.2019.52073.2519

[33] Kumar, K., Kumar, S., Singh, G., Singh, J. P., & Singh, J. (2017). Erosion wear investigation of HVOF sprayed WC-10Co4Cr coating on slurry pipeline materials. *Coatings, 7(4),* 54. https://doi.org/10.3390/coatings7040054

[34] Farokhipour, A., Mansoori, Z., Saffar-Avval, M., & Ahmadi, G. (2018). Numerical modeling of sand particle erosion at return bends in gas-particle two-phase flow. *Transactions B: Mechanical Engineering, Scientia Iranica B, 25(6),* 3231-3242. https://doi.org/10.24200/SCI.2018.50801.1871

[35] Pang, A. L. J., Skote, M., & Lim, S. Y. (2016). Modelling high Re flow around a 2D cylindrical bluff body using the k-ω (SST) turbulence model. *Progress in Computational Fluid Dynamics, An International Journal, 16(1),* 48-57. https://doi.org/10.1504/PCFD.2016.074225

[36] Al-Baghdadi, M. A. R. S. (2015). Applications of computational fluid dynamics and finite element methods in engineering education (Vol. 1). *International Energy and Environment Foundation.*

[37] Finnie, I. (1960). Erosion of surfaces by solid particles. *Wear, 3(2),* 87–103. https://doi.org/10.1016/0043-1648(60)90055-7

[38] McLaury, B. S., Shirazi, S. A., Shadley, J. R., & Rybicki, E. F. (1996). Modelling erosion in chokes. *Proceedings of the ASME Fluids Engineering Summer Meeting,* San Diego, California.

[39] Oka, Y. I., Okamura, K., & Yoshida, T. (2005). Practical estimation of erosion damage caused by solid particle impact. Part 1: Effects of impact parameters on a predictive equation. *Wear, 259,* 95–101. https://doi.org/10.1016/j.wear.2005.01.039

[40] Oka, Y. I., & Yoshida, T. (2005). Practical estimation of erosion damage caused by solid particle impact. Part 2: Mechanical properties of materials directly associated with erosion damage. *Wear, 259,* 102–109. https://doi.org/10.1016/j.wear.2005.01.040

[41] Hamed, A., & Tabakoff, W. (2006). Erosion and deposition in turbomachinery. *Journal of Propulsion and Power, 22(2),* 350-360. https://doi.org/10.2514/1.18462